Influence of the Reference Temperature on the Orientation and Relaxation of Miscible Polystyrene/Poly(vinyl methyl ether) Blends

Christian Pellerin, Isabelle Pelletier, Michel Pézolet, and Robert E. Prud'homme*

Centre de recherche en sciences et ingénierie des macromolécules, Département de chimie, Université Laval, Québec, Canada G1K 7P4

Received July 1, 2002

ABSTRACT: The deformation and relaxation behavior of polymers depends heavily on temperature. In miscible polystyrene/poly(vinyl methyl ether) (PS/PVME) blends, which possess a broad glass transition region, polarization modulation infrared linear dichroism (PM-IRLD) measurements show that when the mean glass transition temperature (T_g) is used as the reference temperature, the orientation and relaxation of orientation of PS in the blends depend significantly on the composition. In contrast, similar values are obtained for blends containing between 40 and 100% PS when the end of the glass transition region (T_{gf}) is used as the reference temperature. Physical aging experiments made by differential scanning calorimetry indicate that T_{gf} can be associated with the highest temperature at which enthalpic relaxation occurs, above the mean T_g of the blend. Both series of results have been analyzed, first, by considering the presence of concentration fluctuations in the miscible blends and, second, in the framework of the Lodge−McLeish model.

Introduction

In studies of the macroscopic deformation and relaxation of polymer blends as a function of composition, a reference temperature has to be chosen. Usually, the glass transition temperature (T_g) is selected for this purpose, and measurements have been done at a given temperature above T_g for several miscible blends, including those of polystyrene (PS) with poly(phenylene oxide) (PPO), poly(vinyl methyl ether) (PVME), and poly(*o*-chlorostyrene) (PoCS).

In PS/PPO blends, the addition of a second component increases the orientation of the matrix.[1,2] The orientation of PPO is always larger than that of PS, but the two polymers relax in a cooperative way with the same characteristic times.[3] In PS/PVME blends, the orientation of PS in the blends increases upon addition of PVME up to 50%.[4,5] PS always possesses a larger orientation than PVME, and the two polymers relax at significantly different rates.[6] In poly(vinylphenol)/poly(ethylene oxide) (PVPh/PEO) blends, Brisson et al. found a maximum orientation of PEO when the composition was around 70% w/w PVPh.[7] In contrast, it was shown by Faivre et al. that the orientation of PS and PoCS is not influenced by the presence of the second component in PS/PoCS blends.[8] Most of these results have been interpreted in terms of variations of the friction coefficient with composition due to the specific interactions between the blend components.

Clearly, different orientation behaviors are often observed as a function of composition when T_g is used as the reference temperature. Furthermore, when a significant broadening of the transition region occurs, which is often if not always the case for polymer blends, the choice of T_g as a reference temperature is problematic. PS/PVME blends constitute an interesting example because this system is completely amorphous and can be prepared in either a miscible or phase-separated state, depending on the preparation conditions.[9,10] It is characterized by a broad glass transition region, and it possesses a lower critical solution temperature (LCST).[11,12] Abtal and Prud'homme have studied PS/PVME blends using the LCST instead of T_g as the reference temperature.[13] They observed a decrease of the orientation of PS upon addition of PVME in the blends when the stretching was performed 62 °C below the LCST. These results were interpreted by an increase of the free volume in the PVME-rich blends.

Infrared linear dichroism (IRLD) has been the most widely used technique for the characterization of orientation of polymer blends because it allows the independent determination of the orientation of each component. However, it suffers from a limited time resolution because two spectra with different polarizations have to be recorded. To overcome this limitation, we have coupled the polarization−modulation (PM) technique to the conventional IRLD. PM-IRLD has made possible the dynamic study of the deformation of polymers and of the light-induced orientation of azopolymers.[14−16]

In this work, we have used PM-IRLD to study the deformation and the relaxation of orientation of PS/PVME blends looking for the most appropriate reference temperature. We propose that the end of the glass transition region (T_{gf}) could be a better choice than the middle of the transition region, as done in previous studies.[1−8] In a first (classical) series of experiments, miscible blends containing between 40 and 100% PS were deformed uniaxially 8 °C above their T_g while, in a second series, they were stretched 4 °C above their T_{gf}. Physical aging experiments were also conducted by differential scanning calorimetry (DSC) to provide further insights into the meaning of T_{gf} and the phase structure of the blends. This opens up the question of the nature of the local environment of a chain segment in a miscible polymer blend.

Experimental Section

Monodisperse atactic polystyrene (Pressure Chemical) with M_w = 942 kg/mol and poly(vinyl methyl ether) (Polymer Scientific Products) with M_w = 59 kg/mol were used. The high-

* Corresponding author: Tel (418) 656-3683; fax (418) 656-7916; e-mail robert.prud'homme@chm.ulaval.ca.

10.1021/ma021035h CCC: $25.00
Published on Web 12/02/2002

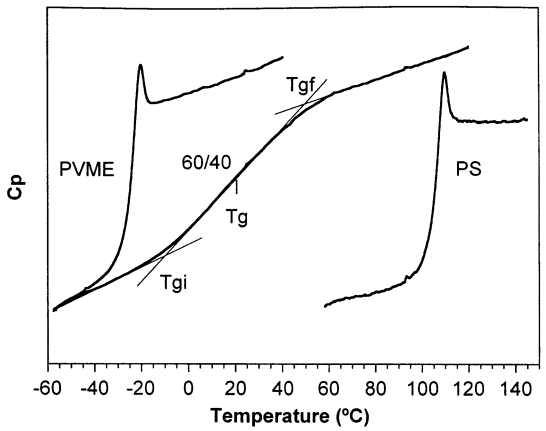

Figure 1. Differential scanning calorimetry traces of pure PS and PVME and of a 60/40 PS/PVME miscible blend. The C_p values (Y scale) have been adjusted to highlight width difference in the transition between the blend and the homopolymers. The initial and final T_g (T_{gi} and T_{gf}) were determined as shown.

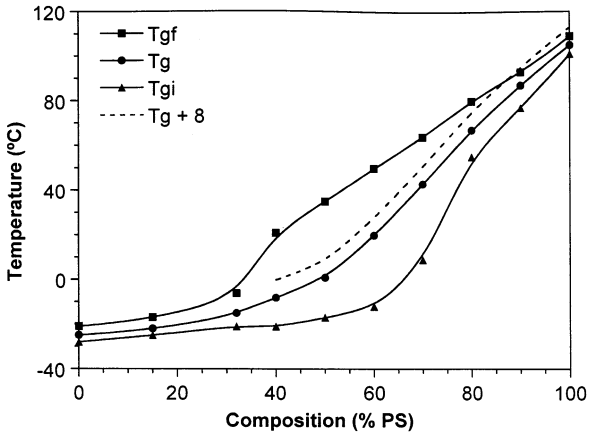

Figure 2. Initial, middle, and final T_g (T_{gi}, T_g, and T_{gf}) as a function of composition in miscible PS/PVME blends. The plain lines are only a guide to the eye, while the dotted line at $T_g + 8$ represents the temperature at which a first series of measurements were made.

and low-molecular-weight fractions of PVME were removed by a series of reprecipitation of benzene solutions of PVME in hexane, a nonsolvent. The polydispersity index of PVME was thus reduced to 1.3, as determined by size exclusion chromatography (Waters model 590) with a light-scattering detector (Wyatt DAWN DSP) in tetrahydrofuran. Self-supported films containing from 40 to 100% w/w PS were cast on glass or Teflon plates from 3% benzene solutions. Films with thicknesses between 30 and 70 μm were used to ensure an absorbance below unity for the infrared bands investigated. Films were air-dried at room temperature for 2 days and then gradually heated under vacuum up to $T_g + 30$ for at least 48 h to remove the last traces of solvent and residual stresses. The samples were cut into strips having 20 mm length and 6 mm width and marked with ink lines to verify the real draw ratio. A pyrotape (Aremco Products #546) was used to avoid slippage of the films during the elongation.

T_g's were determined as the midpoint of the DSC (Perkin-Elmer DSC-7) heat capacity jump at a scanning rate of 10 K/min. The initial and final T_g (T_{gi} and T_{gf}) were determined as the intercept of the baseline with the tangent of the heat capacity jump at low and high temperatures, respectively (see Figure 1). The physical aging experiments were performed on the same apparatus. After a series of three heating scans to remove the thermal history, the sample was quenched and maintained at the annealing temperature for 90 min. After quenching below T_{gi}, two heating scans were run. The difference between the first (annealed) and second (reference) scans allowed the evaluation of the enthalpic relaxation due to the annealing.

PS/PVME films were stretched to a fixed draw ratio of 2 at either $T_g + 8$ or $T_{gf} + 4$ at a constant draw rate of 10 cm/min, using a mechanical stretcher fitted with ZnSe windows to allow the in situ recording of the PM-IRLD spectra during the orientation and relaxation periods. This stretcher, recently constructed in our laboratory, is driven by a stepping motor and can be used to deform samples at draw rates ranging from 10 up to 1200 cm/min, at temperatures between −7 and 170 °C. The temperature was adjusted using an Omega temperature controller (CN 7600) and heating cartridges. For the experiments below room temperature, liquid nitrogen-cooled nitrogen was circulated through the walls of the stretcher. In every case, the samples were held at the deformation temperature for 45 min before stretching, and the temperature control was better than 0.5 °C.

Dichroic difference spectra with a resolution of 8 cm^{-1} were obtained with a Bomem Michelson MB-100 spectrophotometer using the optical setup and the two-channel electronic processing device previously described.[16] A liquid nitrogen-cooled MCT detector (Belov), a ZnSe photoelastic modulator (Hinds PEM-90 type II/ZS50) operating at 50 kHz, a lock-in amplifier (EG&G 7260 DSP) with a 40 μs time constant, and two dual-channel electronic filters (Stanford Research Systems SR650) were used to generate the double modulation and to isolate the experimental signals. All the experiments were conducted in three consecutive acquisition steps: a first series of 180 spectra of four scans was followed by 90 spectra of 30 scans and by a final series of 80 spectra of 75 scans, for a total measurement time of about an hour. At least five samples were deformed under each experimental condition.

The orientation function or order parameter $\langle P_2(\cos\theta)\rangle$ was calculated from the intensity of the dichroic difference, ΔA, as[17]

$$\langle P_2(\cos\theta)\rangle = \frac{2}{3\cos^2\alpha - 1}\frac{\Delta A}{3A_0}\sqrt{\lambda} \qquad (1)$$

where λ is the draw ratio, A_0 the absorbance of the unstretched isotropic sample, and α the average angle between the transition moment of the vibration considered and the main chain axis. The A_0 values were determined from transmission spectra using Nicolet Magna 550 or 750 spectrophotometers.

Results

Figure 1 shows the DSC traces of the pure homopolymers and of a 60/40 PS/PVME blend. A single glass transition is observed for this blend, as well as for the other ones (not shown here), which is normally considered as a proof for miscibility at the scale of the DSC measurement, i.e., 10−20 nm.[18,19] However, it can be observed that PS and PVME exhibit a sharp glass transition, while there is a clear broadening in the 60/40 blend. It has been proposed that this transition broadening can be caused by the presence of concentration fluctuations in the miscible blends at a scale inferior to the spatial resolution of the instrument.[19−24] The effect of such possible heterogeneities will be discussed later in this article.

DSC measurements have been performed at several compositions, and values of the initial, middle, and final T_g's (T_{gi}, T_g, and T_{gf}, respectively) are plotted in Figure 2. The error on T_g and T_{gf} is about ±3 °C in the mid-composition range, while that on T_{gi} is about ±3 °C for the PS- and PVME-rich blends but is larger, up to ±12 °C, for the middle compositions, because its determination is extremely sensitive to the selection of the baseline. A linear decrease of T_g is observed in Figure 2 with the addition of up to 50% PVME in the blends,

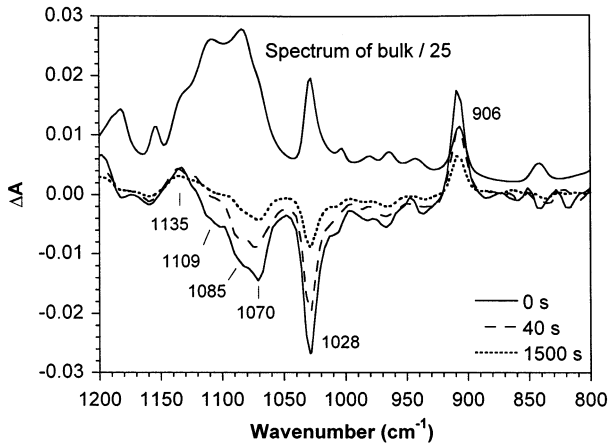

Figure 3. Infrared spectrum of an undeformed 90/10 PS/PVME blend and dichroic difference spectra recorded at the end of the deformation (0 s) and after 40 and 1500 s of relaxation.

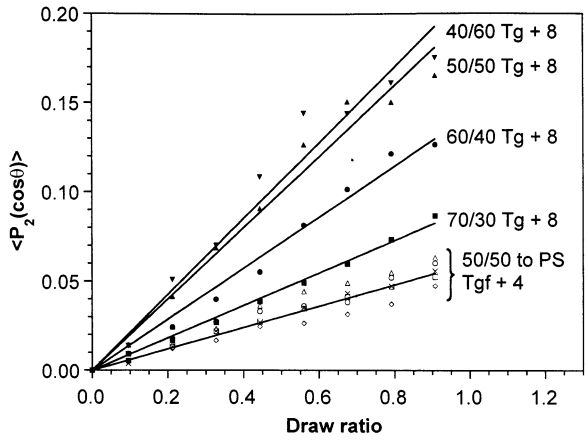

Figure 4. Orientation function $\langle P_2(\cos\theta)\rangle$ of PS in blends containing between 40 and 100% PS as a function of draw ratio λ for deformations at $T_g + 8$ and $T_{gf} + 4$. Filled and hollow symbols of identical shape are used for a given blend composition at $T_g + 8$ and $T_{gf} + 4$, respectively. The data for pure PS (×) are identical at $T_g + 8$ and $T_{gf} + 4$.

followed by a slower decrease in the PVME-rich blends. It was shown that the evolution of T_g in the PVME-rich range can be described by a Kovacs function below a critical fraction of about 55% in PS.[25] T_{gi} remains close to that of pure PVME up to a PS content of about 50%, while T_{gf} shows a more or less linear decrease from pure PS to the 50/50 blend. The width of the transition region varies greatly with composition, and the broader transition is observed in the 60/40 blend with a huge difference between T_{gi} and T_{gf} of 62 K. The maximum difference between the two reference temperatures used in this work, T_g and T_{gf}, is observed in the 50/50 blend in which T_{gf} equals $T_g + 34$.

Figure 3 shows the infrared spectrum of an undeformed 90/10 sample, and three dichroic difference spectra obtained after a deformation at $T_g + 8$, at a stretching rate of 10 cm/min. These spectra were recorded immediately at the end of the deformation (0 s) and after 40 and 1500 s of relaxation. The signal-to-noise ratio of the PM-IRLD spectra is high even if the maximum ΔA is less than -0.03, and the number of scans per spectrum was limited. The acquisition time necessary to obtain the spectra at 0 and 40 s was 1.6 s only. This demonstrates the efficiency of PM-IRLD to follow a rapid kinetics of relaxation. Positive and negative bands are present in the dichroic difference spectra depending on the angle, α, between the transition moment of the vibration considered and the main chain axis, as shown in eq 1. The two well-resolved PS bands observed at 1028 and 906 cm^{-1} are assigned to the ν_{18a} in-plane and ν_{17b} out-of-plane vibrations of the phenyl ring, respectively.[26] These two vibrations are considered to be insensitive to the polymer conformation, and their α angle is 90° and 35°, respectively. Therefore, since the polymer chains orient along the stretching direction during the deformation process, the 906 cm^{-1} band is positive in the dichroic difference spectra while the 1028 cm^{-1} band is negative. In either case, the dichroic difference decreases with time toward zero as the macromolecular chains relax to their isotropic state.

In the spectrum of the bulk sample (Figure 3), the most intense band is located between 1050 and 1150 cm^{-1} and is due to the superposition of at least one PS and three PVME bands. The 1070 cm^{-1} PS band is assigned to the ν'_{18b} vibration, while the 1085, 1109, and 1135 cm^{-1} PVME bands are all associated with the C−O−C stretching of the methoxy side chain. It is worth noting that, in the infrared spectrum of the bulk sample, the 1070 cm^{-1} PS band appears as a weak shoulder on the PVME bands, while it is stronger than the PVME bands in the dichroic difference spectra. This indicates that, during the deformation of this blend, the chains of PVME remain poorly oriented as compared to those of PS. In a previous work, the 2820 cm^{-1} band, assigned to the symmetric CH_3 stretching of the methoxy group, has been used to follow the orientation and relaxation dynamics of PVME in PS/PVME blends.[6] It was noted that the orientation of PVME is always smaller than that of PS and that the two polymers relax with different relaxation times.

The chain order parameter $\langle P_2(\cos\theta)\rangle$ of PS can be determined quantitatively using eq 1 from the dichroic difference intensity of the 906 or 1028 cm^{-1} bands. Since identical trends were observed with these two bands, only the results using the latter will be shown. Figure 4 shows the variation of $\langle P_2(\cos\theta)\rangle$ with draw ratio during the deformation of PS/PVME blends containing between 40 and 100% PS deformed at either $T_g + 8$ (filled symbols) or $T_{gf} + 4$ (open symbols). Since $T_{gf} + 4$ is equivalent to $T_g + 8$ for pure PS, the results of the different blends under the two deformation conditions can be compared with a single set of PS results. A linear increase of $\langle P_2(\cos\theta)\rangle$ with the draw ratio is found for all samples, although a certain leveling seems to appear at higher draw ratios in the 40/60 blend deformed at $T_g + 8$. However, this can be merely the effect of the scatter in the data caused by the small dichroic difference (the maximum value before relaxation is typically below 0.01) due to the low absorbance of PS in this PVME-rich blend. Moreover, the intense infrared band in the 1050−1150 cm^{-1} region is saturated, which causes some baseline drifts. As expected, the $\langle P_2(\cos\theta)\rangle$ values determined during the deformations at $T_{gf} + 4$ are smaller than those at $T_g + 8$ for the same blend composition because the orientation function of a polymer decreases with temperature.[26,27]

When T_g is used as the reference temperature, the addition of more than 10% PVME to the blends leads to an important increase of the order parameter, the orientation of PS in the 50/50 blend being almost 3 times

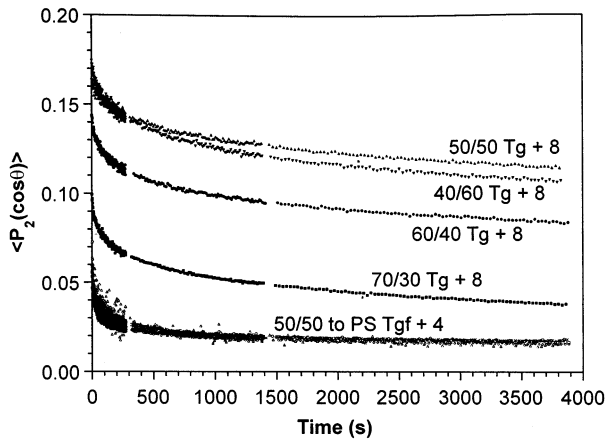

Figure 5. Relaxation curves of PS in blends containing between 40 and 100% PS as a function of time after deformations at $T_g + 8$ or $T_{gf} + 4$. Filled and hollow symbols of identical shape are used for a given blend composition at $T_g + 8$ and $T_{gf} + 4$, respectively. The data for pure PS (×) are identical at $T_g + 8$ and $T_{gf} + 4$.

larger than that in the pure homopolymer, in agreement with our previous measurements at $T_g + 15$[6] and with those of Abtal and Prud'homme, in which a maximum orientation was observed in the 50/50 blend.[4] On the other hand, Figure 4 shows that when T_{gf} is used as a reference temperature, a single straight line reasonably describes the evolution of all blends of composition between 50 and 100% PS at $T_{gf} + 4$.

Figure 5 shows the relaxation curves of PS in the different blends after their deformation at $T_g + 8$ and $T_{gf} + 4$. Different relaxation regimes are seen in these curves. A fast decay is observed at short times, while a slow chain relaxation occurs at longer times. It was shown that at least three separate relaxation times must be considered in the analysis of these curves.[15] When T_g is used as the reference temperature, the relaxation rate seen in Figure 5 is faster in pure PS than in the blends; i.e., the increase of PVME content leads to an important modification of the relaxation rate of PS, at short and long relaxation times, especially for PVME-rich blends. However, this effect reaches a maximum at about 50% PVME since the relaxation of the 40/60 blend is faster than that of the 50/50 blend, in contrast with the behavior of the two samples during deformation where a similar orientation of the two blends was observed within experimental error (see Figure 4). This discrepancy is probably an artifact due to the higher dispersion of the data in the deformation curves. When the measurements are performed during the stretching, some baseline fluctuations can occur in the spectra, which is not the case during the relaxation because the film is static.

A variation of the friction coefficient with composition has been proposed in the literature to explain the deformation behavior of polymer blends[1,28−31] in general and of PS/PVME blends in particular.[4,5] NMR[32] and infrared[33] spectroscopies have been used to demonstrate the presence of specific interactions between the phenyl group of PS and the oxygen of the methoxy group of PVME. These interactions lead to a small negative interaction parameter, which explains the miscibility of the blends.[34] If the temperature is kept constant relative to the blend's T_g (but not at a constant absolute temperature), it can be argued that when the number of interacting units increases, i.e., when the fraction of PVME in the blend becomes larger, the friction coefficients of PS and PVME should increase, thus leading to a hindered relaxation of the polymers. Such a behavior is indeed observed in Figure 5 for PS in the blends when T_g was used as the reference temperature and was shown to occur for PVME in blends containing up to 40% PVME.[6]

However, these interactions are expected to reach a maximum near a 1:1 ratio of interacting units, which corresponds to a blend containing about 64 wt % PS. This phenomenon was observed in miscible blends of PVPh with several polymers[7,28] but not in the current study. Indeed, the hindering effect of PVME increases beyond the 1:1 ratio of interacting units since a maximum orientation is observed for blends containing 50% PS and not around 64% PS. This means that, even if the specific interactions play a role in the orientation behavior of PS/PVME blends, other factors must be taken into account. A variation of the entanglement density with composition has also been invoked in the literature to explain deformation results in some polymer blends.[2,35] Since the entanglement density of PVME is higher than that of PS (8500 g/mol between entanglement points for PVME as compared to 18 000 g/mol for PS[36]), the addition of PVME in PS could increase the density of the topological network of the PS chains, thus leading to a hindered relaxation. In this framework, however, a maximum of the orientation function is not expected since the addition of larger amounts of PVME should increase even more the entanglement density.

In contrast, it is obvious in Figure 5 that the relaxation curves of PS and of blends containing up to 50% PVME are very similar when the deformation temperature is $T_{gf} + 4$. (The data of the 40/60 blend are not shown because their larger scatter masks the similarity of the other curves.) In Figure 5, the orientation function of the different blends at the end of the deformation ($t = 0$ s) is very close at $T_{gf} + 4$, and the $\langle P_2(\cos\theta)\rangle$ values at long relaxation times are identical. In principle, $\langle P_2(\cos\theta)\rangle$ values should decrease until the sample is isotropic, but the reptation time for high-molecular-weight PS is much longer than the experimental measurement time at such temperatures. The behavior at short times (less than 300 s) still appears to be influenced by the composition of the blend, the orientation of the 50/50 blend being slightly higher than that of the 70/30 blend, which also possesses a slightly larger $\langle P_2(\cos\theta)\rangle$ than pure PS. The results of Figures 4 and 5 suggest that T_{gf} could be a useful reference temperature to compare the relaxation curves of miscible polymer blends. Apart from the fact that the orientation and relaxation curves are very similar for all blends, the use of T_{gf} as a reference temperature takes into account the broadening of the glass transition region. These results are in agreement with those of Kim and Son, who have investigated the rheology of miscible PS/PVME blends using T_{gi}, T_g, and T_{gf} as reference temperatures.[37] They have observed a milder variation of the zero-shear viscosity when T_{gf} was used as the reference temperature and have concluded that the dynamics of the chains do not follow the average mobility of the blend at T_g.

A further demonstration of the interest of T_{gf} as a reference temperature for the deformation of miscible polymer blends is shown in Figure 6. In this figure, the slope of the deformation curves ($\Delta\langle P_2(\cos\theta)\rangle/\Delta\lambda$), such as those shown in Figure 4, is plotted as a function of the difference between the deformation temperature and

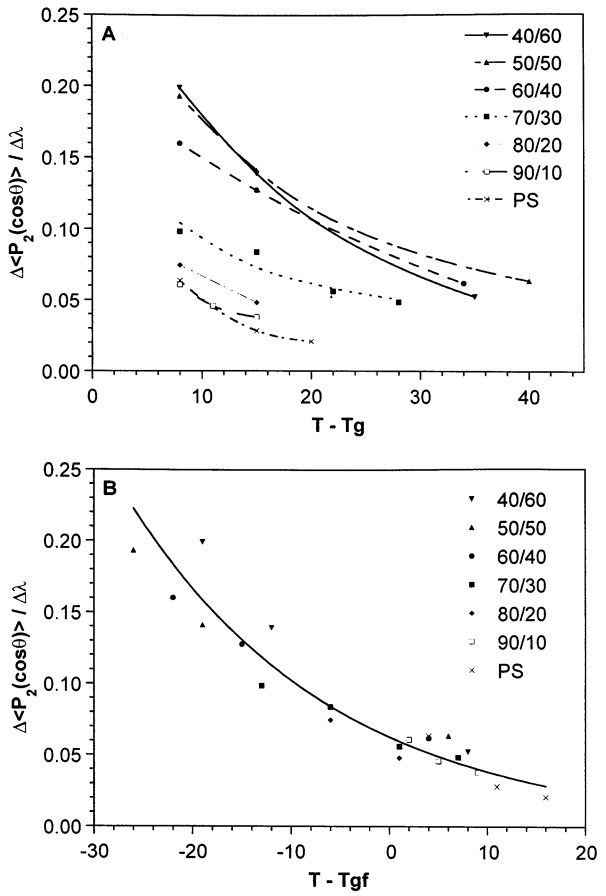

Figure 6. Slope of the deformation curves ($\Delta\langle P_2(\cos\theta)\rangle/\Delta\lambda$) as a function of the relative deformation temperature ($T - T_{ref}$) using (A) T_g as the reference temperature and (B) T_{gf} as the reference temperature.

the reference temperature ($T - T_{ref}$). The data were obtained over a wide range of temperatures, from $T_g + 8$ to $T_g + 40$. In Figure 6A, the reference temperature is considered to be T_g. It can be observed that, as the deformation temperature becomes closer to T_g, a significant increase in the slope of the deformation curves occurs for all blends, in agreement with the expected behavior.[26,27] A larger orientation is found at any given distance from T_g when the PVME content in the blends increases, with the exception of the 40/60 blend for reasons already discussed. In contrast, Figure 6B shows that, when T_{gf} is used as the reference temperature, similar slopes are obtained for pure PS and for PS in all the blends for deformation temperatures ranging from about $T_{gf} - 25$ to $T_{gf} + 15$. It should be noticed that the line drawn is only a guide for the eye and does not have any theoretical meaning. A scatter is noticed in Figure 6B at low temperatures relative to T_{gf}, but this is only caused by the 40/60 blend, for which the error on the deformation slope is larger than that of the other samples.

This empirical correlation indicates that the results of Figures 4 and 5 at $T_{gf} + 4$ are not fortuitous and that T_{gf} could indeed be considered as a relevant reference temperature for miscible polymer blends. One could also consider plotting the results of Figure 6B as a function of $(T - T_{gf})/(T_{gf} - T_{gi})$ instead of $T - T_{gf}$ to take into account the total width of the glass transition. Such a representation (not shown) also gives a reasonable correlation, but it was not retained because this function is too much affected by the error in the determination of T_{gi}, which is much larger than that for T_{gf}.

In an attempt to provide a physical meaning to T_{gf} and to seek new insights into the behavior of PS/PVME blends, we have performed physical aging experiments by DSC. In a typical experiment, the sample was annealed at different temperatures below T_g for a given time. Since no large-scale motions of the chains should occur below T_g, the glassy sample densifies and minimizes its free volume and enthalpy until it reaches (in theory) its equilibrium state.[38−40] In practice, kinetic effects due to the high viscosity of polymers below T_g limit the enthalpy loss during the annealing at very low temperatures. According to the free volume model, a chain segment can relax if and only if the available free volume is larger than a critical volume defined by the cooperative length of the segment.[41] A temperature T_0, at which the free volume vanishes and no conformation rearrangements can occur, is often considered to be about 50 °C below the experimental T_g as determined by DSC.[42] On the other hand, annealing above T_g should have no effect since the free volume is large and the molecular motions are fast enough to reach the liquid-like equilibrium.

After annealing at any given temperature, the sample was further quenched, and two heating scans were performed. In the first one, the enthalpy lost during the annealing was recovered when T_g was attained, and an enthalpic relaxation peak was observed on the DSC trace. The sample was then rapidly quenched much below T_{gi}, and the second scan was immediately made and thus presented no annealing effect. The difference between the two scans allows the determination of the enthalpic relaxation as a function of annealing time and temperature.

Figure 7 shows physical aging experiments on pure PS at temperatures between $T_g - 30$ and $T_g + 10$ for a constant annealing time of 90 min. Figure 7A shows the first heating scan after the annealing, and Figure 7B shows the difference between the first and second heating scans. Large enthalpic relaxation peaks can be observed for annealing performed at $T_g - 10$ and $T_g - 20$, while a small broad peak is noticed after an annealing at $T_g - 30$. When the annealing is done at $T_g + 10$, no relaxation occurs at all, which is expected since the polymer is not glassy. On the other hand, it is interesting to observe the presence of a small but significant and reproducible peak when the aging is performed exactly at T_g. Additional annealings were then made a few degrees above T_g, and it was realized that the last traces of enthalpic relaxation vanished at about $T_g + 4$, which corresponds to the T_{gf} as determined on the DSC traces.

Similar measurements were performed on the different PS/PVME blends, and Figure 8 shows the results obtained for the 60/40 blend. Because of the important broadening of T_g in the blends, the relaxation peaks are not as clear in Figure 8A as in Figure 7A. However, the difference curves of Figure 8B clearly reveal that significant enthalpic relaxation occurs at temperatures as low as $T_g - 40$ and as high as $T_g + 20$. Peaks obtained after annealing at a low temperature are observed in the middle of the heat-capacity jump and not close to T_g.[43] Such peaks were also observed in blends of PMMA with poly(epichlorhydrin) (PECH) and were associated with the presence of a microphase rich in PECH relaxing at low temperature.[44] As observed with pure

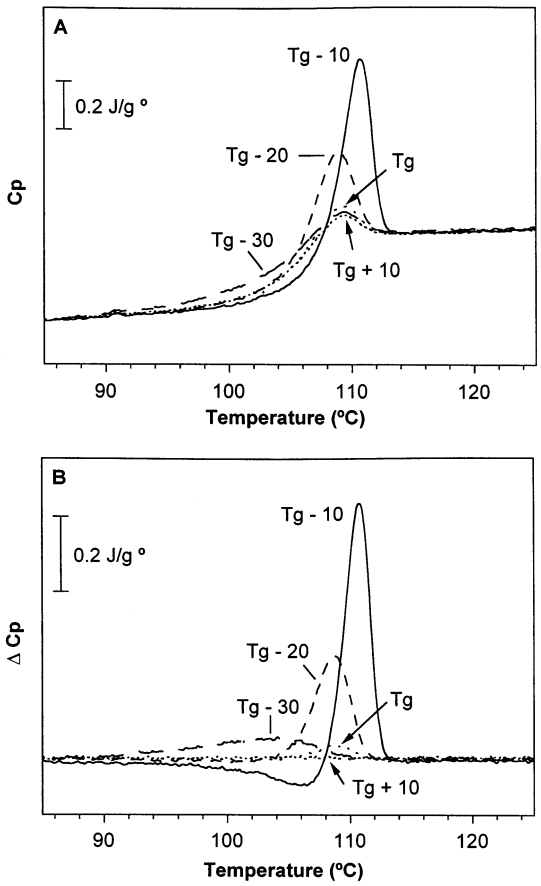

Figure 7. Physical aging experiments on pure PS at temperatures ranging from $T_g - 30$ to $T_g + 10$: (A) first DSC scan following a 90 min annealing; (B) difference between the first and second DSC scans following annealing.

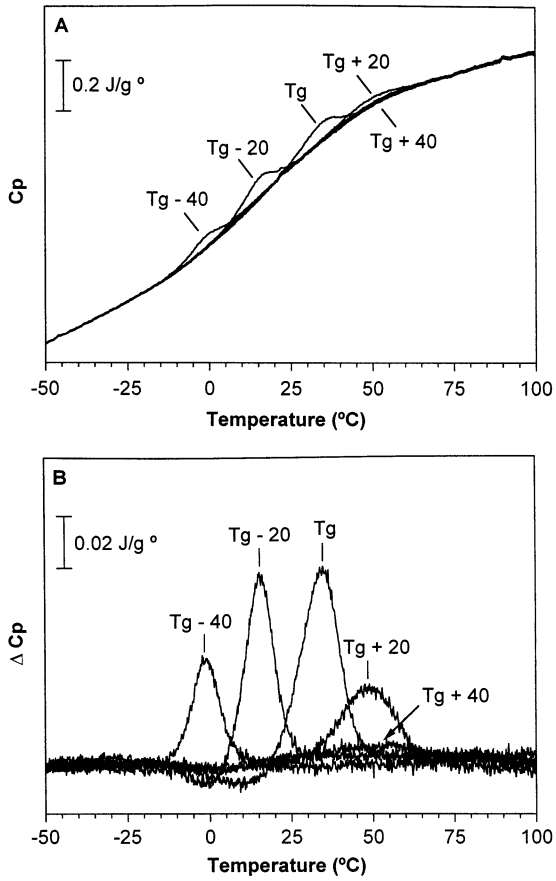

Figure 8. Physical aging experiments on a 60/40 PS/PVME miscible blend at temperatures ranging from $T_g - 40$ to $T_g + 40$: (A) first DSC scan following a 90 min annealing; (B) difference between the first and second DSC scans following annealing.

PS, the last trace of enthalpic relaxation occurs close to T_{gf}, at an extrapolated annealing temperature of about $T_g + 30$ for the 60/40 blend. A similar conclusion can be drawn from the measurement with the other blends. These measurements thus indicate that T_{gf} is the highest temperature at which enthalpic relaxation can occur after annealing.

Discussion

It has recently been reported that the dynamics responsible for physical aging in polystyrene are spatially heterogeneous and that regions of different mobility age at different rates.[45] The enthalpic relaxation peak of pure PS, following an annealing slightly above T_g, could thus be related to a distribution of density in the material. However, a density effect cannot explain the enthalpic relaxation observed for the 60/40 blend at $T_g + 20$. As mentioned earlier, the presence of concentration fluctuations has been suggested to explain the broadening of the transition region in miscible PS/PVME blends.[20] The broadening of the dielectric loss peak in these blends has also been associated with a distribution of microenvironments,[9,46] while rheology studies have demonstrated the thermorheological complexity of the blend.[47] From numerous NMR experiments, it has also been proposed that the globally miscible PS/PVME blends could be heterogeneous at the segmental scale. As early as 1974, Kwei et al. have suggested from spin−spin and spin−lattice relaxation measurements that so-called miscible blends were extensively mixed but still microheterogeneous at a segmental scale.[48] Chu et al. have also used spin−lattice relaxation techniques and have measured heterogeneities of at least 1 nm in PS/PVME blends,[49] while Schmidt-Rohr et al. have reported the presence of dynamic heterogeneities of 3.5 nm by wide-line separation measurements.[50]

Different models have been developed to take into account the complexity of the relaxation in polymeric systems. Zetsche and Fischer have considered the case of a miscible blend with a symmetric distribution of concentration fluctuations around the mean composition.[51] They have proposed that domains of similar volumes are formed, and each domain of local composition ϕ_{loc} is characterized by a local T_g ($T_{g,loc}$) corresponding to the macroscopic T_g of a blend of corresponding composition ϕ. Kumar et al. have refined that model in order to take into account a cooperative volume that depends on the local composition of the domains.[52] This model can explain the presence of a bimodal distribution of dynamic concentration fluctuations observed in some polymer blends, in which domains of almost pure low-T_g polymer coexist with regions with concentration fluctuations centered around the mean composition. It was also suggested that the presence of strong specific interactions between the components or a small difference between the T_g of the pure polymers should lead to a thermorheologically simple blend, without dynamic heterogeneities.

These models appear to be qualitatively consistent with the results obtained in this work. In the framework

of the Zetsche−Fischer model, PS/PVME blends could be considered as composed of nanodomains with a continuous variation of composition and $T_{g,loc}$. When physical aging experiments are performed above the mean T_g of the blend, domains rich in PS would still be below their $T_{g,loc}$ and could relax, giving rise to the enthalpic relaxation peaks at temperatures up to T_{gf}. In this framework, T_{gf} could be considered as the highest local T_g in this specific blend (without considering the density effect). Similarly, T_{gi} would be representative of the local T_g of domains with the largest concentration of the low-T_g polymer.

In this context, it is not surprising to observe a significant annealing effect in the 60/40 blend at $T_g - 40$ since this temperature is about 8 °C only below T_{gi}. Since T_{gf} and T_{gi} of the 60/40 blend are 50 and −12 °C, respectively, this would lead to PS-rich and PVME-rich domains with local compositions ranging between approximately 72/28 and 35/65. This distribution is not symmetric around the mean value of 60/40 and is broader in the low-T_g range. Furthermore, the observation that T_{gi} is only slightly higher than the T_g of pure PVME for blends containing up to 50% PS in Figure 2 could be interpreted as a bimodal distribution with domains very rich in PVME in addition to a distribution of concentration fluctuations centered around the mean composition, as described in the Kumar model.[52] It must be emphasized, though, that the uncertainty in the determination of T_{gi} in the blends is larger than that of T_g and T_{gf}.

As mentioned earlier, the orientation function of a polymer decreases with the drawing temperature. In the Doi−Edwards model for the relaxation of entangled polymers, the three characteristic relaxation times are inversely proportional to temperature.[53] As a consequence, a shift in temperature of a few degrees has a much larger effect close to T_g than far from it. The orientation function of samples deformed at $T_g + 25$ and $T_g + 30$ may be similar, while a larger difference is expected if the deformations are performed at $T_g + 5$ and $T_g + 10$. A sample deformed below T_g would give a very high orientation as compared to one deformed in the rubbery state.

Assuming that miscible PS/PVME blends are composed of a distribution of microenvironments with different local compositions, a certain number of domains with a larger amount of high-T_g polymer will still be below their $T_{g,loc}$ when the deformation is performed a few degrees above the mean macroscopic T_g. This can be the case when T_g is used as the reference temperature, and the deformation is performed at $T_g + 8$. This is shown in Figure 2, in which $T_g + 8$ is drawn as a dotted line. For the 90/10 blend, $T_g + 8$ is already above T_{gf}, so all the domains can be considered in the rubbery state. However, for blends with 20% or more PVME, the distribution of $T_{g,loc}$ extends beyond the deformation temperature. Such domains are still "frozen" in the glassy state and cannot relax as freely as in the rubbery state. This leads to a higher orientation during the deformation of the blends and to a slower relaxation dynamics.

Since the maximum difference between T_g and T_{gf} is observed in the 50/50 blend, it is not surprising to observe the higher $\langle P_2(\cos\theta)\rangle$ values with this specific blend because it should contain domains with $T_{g,loc}$ far away from the deformation temperature and presumably the largest fraction of domains below their $T_{g,loc}$. In the 40/60 blend, the distribution of environments becomes narrower, and the relaxation rate is accordingly faster than in the 50/50 blend. On the other hand, when the polymers are deformed using T_{gf} as the reference temperature, all the domains are necessarily above their $T_{g,loc}$, so the orientation relaxation is relatively rapid and similar in these rubbery samples. The slower relaxation rates still observed at short times in the polymer blends with a larger PVME fraction in Figure 5 are probably caused by a combined effect of the specific interactions and of the increased entanglement density.

Recently, Lodge and McLeish have proposed a new model (L−M model) providing an explanation for several experimental results that were previously explained by the presence of concentration fluctuations, but without involving such heterogeneities.[54] They postulated that the relevant length scale for the monomeric friction coefficient or other local probes is primarily determined by the Kuhn length of the chain, l_k. The relaxation of the chain segments is thus influenced by the concentration of repeat units within a volume V proportional to l_k^3. This volume depends weakly on temperature, in contrast with the models of Zetsche and Fischer, and of Kumar et al., in which the cooperative volume is related to $(T - T_0)^{-2}$ and thus diverges at the Vogel temperature T_0. In the L−M model, the self-concentration effect is also taken into account, since the region surrounding an A unit in an A/B polymer blend is, on average, enriched in the A component as compared to the bulk composition, simply due to the chain connectivity. The effective local composition ϕ_{eff} experienced by an A repeat unit is thus given by

$$\phi_{eff} = \phi_s + (1 - \phi_s)\phi \tag{2}$$

where ϕ_s is the self-concentration factor, determined from experimentally available values as

$$\phi_s = \frac{C_\infty M_0}{k\rho N_{av} V} \tag{3}$$

where C_∞ is the chain characteristic ratio, M_0 the molar mass of the repeat unit, k the number of bonds per repeat unit, ρ the density, and N_{av} the Avogadro number.

Using their model, Lodge and McLeish have made successful comparisons with experimental results for several miscible blends.[54] For example, the effective T_g of the two components in blends of PS with poly(tetramethyl carbonate), which were determined as the temperature at which the monomeric friction factor was 22.5 dyn s/cm, has been qualitatively predicted. Similarly, the L−M model predicts the T_g broadening in polymer blends without requiring concentration fluctuations, including a larger transition for blends rich in the high-T_g component than for those rich in the low-T_g component. The model was also successfully applied to PS/PVME blends, for which a nearly quantitative agreement was obtained between the predictions and the effective T_g of PVME, as determined from the relaxation time by dielectric spectroscopy, in a large composition range.[55]

In this context, T_{gf} can be related to the effective T_g of PS, while T_{gi} could be associated with that of PVME. Indeed, a general agreement is found between the effective local composition of PS and PVME as calculated with the L−M model and those estimated from

the experimental values of T_{gi} and T_{gf}. This is especially true for PS in the blends, while the self-concentration of PVME appears to be overestimated when the blends contain more than 80% in PS. In the 60/40 blend, local compositions of 72/28 and 35/65 have been estimated from T_{gf} and T_{gi}, as mentioned earlier, while ϕ_{eff} values calculated with eqs 2 and 3 are 71/29 and 45/55 for PS and PVME repeat units, respectively. The L−M model could thus explain, at least in part, the glass transition broadening in miscible PS/PVME blends. Several factors can account for the quantitative differences between those values, for instance the uncertainty on the experimental DSC results or on the reference data used for the calculations, or the choice of a discrete cubic volume in eq 3, which could be replaced by a sphere, or the consideration of an exponential decay rather than a sharp frontier. Foremost, a simple equivalence is not expected between ϕ_{eff} and the compositions estimated from T_{gf} and T_{gi} since even pure polymers possess a T_g breadth of about 8 °C.

Considering the L−M model, it is not surprising to observe similar orientation and relaxation curves for all blends when T_{gf} is used as the reference temperature because all deformations would be performed at a comparable temperature relative to the effective T_g of PS in the blend. Deformations performed above T_{gi}, at a temperature relative to the effective T_g of PVME in the blends, could also yield similar relaxation curves for PVME in the blends. The L−M model thus constitutes an attractive approach to explain several of the experimental results by removing the necessity to consider the presence of concentration fluctuations in the miscible blends. However, it does not fully explain the physical aging results since enthalpic relaxation peaks should appear close to either T_{gi} or T_{gf} if PS and PVME would both feel a discrete effective T_g in the blends. In contrast, the peaks observed in Figure 8 after annealing at temperatures close to T_g clearly appear in the middle of the transition, a phenomenon that was previously related to nanoheterogeneities.[44] A distribution of local concentration fluctuations could thus act as a supplementary factor superimposed on the self-concentration effect.

The interpretation of the present results is in agreement with results obtained in the literature for immiscible PS/PVME blends. Abtal and Prud'homme have studied the orientation of phase-separated PS/PVME blends and have shown that the orientation of PS is higher in the immiscible than in the miscible blends when the T_g of the miscible blend is taken as the reference temperature.[56] They explained this result by considering that the sample was deformed below the T_g of the PS-rich phase, thus inducing a high orientation in these glassy regions. This is in line with the present results: in terms of the concentration fluctuation model, a larger difference between the deformation temperature and $T_{g,loc}$ is expected when the degree of phase separation increases from nanoheterogeneities to macrophases, leading to a higher orientation of PS. In terms of the L−M model, phase separation should increase the effective T_g of PS as compared to that in the miscible blend, also leading to a higher orientation.

As mentioned earlier for PS/PPO blends, an increase of the orientation of PS and PPO was observed when PPO was added to the matrix.[1−3] This behavior could be associated with the increase of the glass transition width, which doubles in the mid-composition range as compared to those of pure PS and PPO. The orientation increase is smaller in this system than in PS/PVME blends, which exhibits a larger T_g broadening. The increase in orientation of PPO when the blends are deformed at a given temperature relative to T_g could easily be explained by considering either concentration fluctuations or the L−M model using the arguments presented for PS in this article. However, the increase in the orientation of PS does not appear to be solely explained by the L−M model, since the distance from its effective T_g should increase by adding PPO to the system. It could be due to a combined effect of nanoheterogeneities, friction coefficient, or entanglement density variations, and experimental data on a wider composition range could allow a better understanding of the orientation of this system. On the other hand, the T_g's of PS and PoCS are close such that the transition broadening is more limited in these miscible blends, therefore explaining the absence of significant composition effect on the orientation of the blends.[8]

Conclusions

The choice of a reference temperature has a major impact on the deformation and relaxation behavior of miscible polymer blends possessing a broad glass transition region. When T_g is used as the reference temperature, the orientation of PS in miscible PS/PVME blends increases and its relaxation rate decreases by adding PVME in blends containing more than 50 wt % of PS. This trend is inverted for blends containing less than 50% of PS, an effect that does not seem to be fully explained considering only friction coefficient and entanglement density variations. In contrast, very similar orientation and relaxation results are observed for blends containing between 40 and 100% PS when T_{gf} is used as the reference temperature. Physical aging results indicate that enthalpic relaxation can be observed above T_g for miscible polymer blends with a broad glass transition, a fact that can have several consequences on their practical use, and that T_{gf} is the highest temperature at which it occurs. These results were interpreted using two different frameworks. First, the presence of a large distribution of concentration fluctuations around the mean composition could explain both the orientation and physical aging experiments; T_{gf} would, in that case, be related to the highest local T_g (associated with the highest local concentration in PS) in the blend. Second, T_{gf} would be associated with the effective T_g experienced by PS in the blends in the framework of the Lodge−McLeish model; this model can nicely explain the orientation and relaxation results without the need of introducing spatial heterogeneities, but it does not fully account for the physical aging results.

Acknowledgment. This work was supported by NSERC of Canada and FCAR of the Province of Québec. C.P. and I.P. also express their thanks to NSERC and FCAR for postgraduate scholarships and to G. Guérin for several helpful discussions.

References and Notes

(1) Lefebvre, D.; Jasse, B.; Monnerie, L. *Polymer* **1981**, *22*, 1616.
(2) Zhao, Y.; Prud'homme, R. E.; Bazuin, C. G. *Macromolecules* **1991**, *24*, 1261.
(3) Messé, L.; Prud'homme, R. E. *J. Polym. Sci., Part B: Polym. Phys.* **2000**, *38*, 1405.
(4) Abtal, E.; Prud'homme, R. E. *Macromolecules* **1994**, *27*, 5780.

(5) Faivre, J. P.; Jasse, B.; Monnerie, L. *Polymer* **1985**, *26*, 879.
(6) Pellerin, C.; Prud'homme, R. E.; Pézolet, M. *Macromolecules* **2000**, *33*, 7009.
(7) Rinderknecht, S.; Brisson, J. *Macromolecules* **1999**, *32*, 8509.
(8) Faivre, J. P.; Xu, Z.; Halary, J. L.; Jasse, B.; Monnerie, L. *Polymer* **1987**, *28*, 1881.
(9) Bank, M.; Leffingwell, J.; Thies, C. *Macromolecules* **1971**, *4*, 44.
(10) Djordjevic, M. B.; Porter, R. S. *Polym. Eng. Sci.* **1982**, *22*, 1109.
(11) Nishi, T.; Wang, T. T.; Kwei, T. K. *Macromolecules* **1975**, *8*, 7.
(12) Polios, I. S.; Soliman, M.; Lee, C.; Gido, S. P.; Schmidt-Rohr, K.; Winter, H. H. *Macromolecules* **1997**, *30*, 4470.
(13) Abtal, E.; Prud'homme, R. E. *Polymer* **1993**, *34*, 4661.
(14) Pézolet, M.; Pellerin, C.; Prud'homme, R. E.; Buffeteau, T. *Vib. Spectrosc.* **1998**, *18*, 103.
(15) Messé, L.; Pézolet, M.; Prud'homme, R. E. *Polymer* **2001**, *42*, 563.
(16) Buffeteau, T.; Pézolet, M. *Appl. Spectrosc.* **1996**, *50*, 948.
(17) Lafrance, C.-P.; Nabet, A.; Prud'homme, R. E.; Pézolet, M. *Can. J. Chem.* **1995**, *73*, 1497.
(18) Miller, J. B.; McGrath, K. J.; Roland, C. M.; Trask, C. A.; Garroway, A. N. *Macromolecules* **1990**, *23*, 4543.
(19) MacKnight, W. J.; Karasz, F. E.; Fried, J. R. Solid State Transition Behavior of Blends. In *Polymer Blends*; Paul, D. R., Newman, S., Eds.; Academic Press: New York, 1978; Vol. 1, p 185.
(20) Bershtein, V. A.; Egorova, L. M.; Prud'homme, R. E. *J. Macromol. Sci., Phys.* **1997**, *B36*, 513.
(21) Bershtein, V. A.; Yakushev, P. N.; Karabanova, L.; Sergeeva, L.; Pissis, P. *J. Polym. Sci., Part B: Polym. Phys.* **1999**, *37*, 429.
(22) Chang, G.-W.; Jamieson, A. M.; Yu, Z.; McGervey, J. D. *J. Appl. Polym. Sci.* **1997**, *63*, 483.
(23) Cowie, J. M. G.; Harris, S.; Ribelles, J. L. G.; Meseguer, J. M.; Romero, F.; Torregrosa, C. *Macromolecules* **1999**, *32*, 4430.
(24) Urakawa, O.; Fuse, Y.; Hori, H.; Tran-Cong, Q.; Yano, O. *Polymer* **2001**, *42*, 765.
(25) Aubin, M.; Prud'homme, R. E. *Polym. Eng. Sci.* **1988**, *28*, 1355.
(26) Jasse, B.; Koenig, J. L. *J. Polym. Sci., Polym. Phys. Ed.* **1979**, *17*, 799.
(27) Lefebvre, D.; Jasse, B.; Monnerie, L. *Polymer* **1983**, *24*, 1240.
(28) Li, D.; Brisson, J. *Macromolecules* **1997**, *30*, 8425.
(29) Zhao, Y.; Jasse, B.; Monnerie, L. *Polymer* **1989**, *30*, 1643.
(30) Saito, H.; Takahashi, M.; Inoue, T. *J. Polym. Sci., Part B: Polym. Phys.* **1988**, *26*, 1761.
(31) Bazuin, C. G.; Fan, X.-D.; Lepilleur, C.; Prud'homme, R. E. *Macromolecules* **1995**, *28*, 897.
(32) Mirau, P. A.; White, J. L.; Heffner, S. A. *Macromol. Symp.* **1994**, *86*, 181.
(33) Garcia, D. *J. Polym. Sci., Polym. Phys. Ed.* **1984**, *22*, 107.
(34) Han, C. C.; Bauer, B. J.; Clark, J. C.; Muroga, Y.; Matsushita, Y.; Okada, M.; Tran-cong, Q.; Chang, T.; Sanchez, I. C. *Polymer* **1988**, *29*, 2002.
(35) Kawabata, K.; Fukuda, T.; Tsujii, Y.; Miyamoto, T. *Macromolecules* **1993**, *26*, 3980.
(36) Chun, B. C.; Gibala, R. *Polymer* **1994**, *35*, 2256.
(37) Kim, J. K.; Son, H. W. *Polymer* **1999**, *40*, 6789.
(38) Cowie, J. M. G.; Ferguson, R. *Macromolecules* **1989**, *22*, 2307.
(39) Brunacci, A.; Cowie, J. M. G.; Ferguson, R.; McEwen, I. J. *Polymer* **1997**, *38*, 865.
(40) Struik, L. C. E. *Physical Aging in Amorphous Polymers and Other Materials*; Elsevier Scientific Pub. Co.: Amsterdam, 1978.
(41) Turnbull, D.; Cohen, M. H. *J. Chem. Phys.* **1961**, *34*, 120.
(42) Adam, G.; Gibbs, J. H. *J. Chem. Phys.* **1965**, *43*, 139.
(43) Cowie, J. M. G.; Ferguson, R. *Macromolecules* **1989**, *22*, 2312.
(44) Clark, J. N.; Fernandez, M. L.; Tomlins, P. E.; Higgins, J. S. *Macromolecules* **1993**, *26*, 5897.
(45) Thurau, C. T.; Ediger, M. D. *J. Chem. Phys.* **2002**, *116*, 9089.
(46) Roland, C. M.; Ngai, K. L. *Macromolecules* **1992**, *25*, 363.
(47) Pathak, J. A.; Colby, R. H.; Floudas, G.; Jérome, R. *Macromolecules* **1999**, *32*, 2553.
(48) Kwei, T. K.; Nishi, T.; Roberts, R. F. *Macromolecules* **1974**, *7*, 667.
(49) Chu, C. W.; Dickinson, L. C.; Chien, J. C. W. *J. Appl. Polym. Sci.* **1990**, *41*, 2311.
(50) Schmidt-Rohr, K.; Clauss, J.; Spiess, H. W. *Macromolecules* **1992**, *25*, 3273.
(51) Zetsche, A.; Fischer, E. W. *Acta Polym.* **1994**, *45*, 168.
(52) Kumar, S. K.; Colby, R. H.; Anastasiadis, S. H.; Fytas, G. *J. Chem. Phys.* **1996**, *105*, 3777.
(53) Doi, M. *J. Polym. Sci., Polym. Phys. Ed.* **1980**, *18*, 1005.
(54) Lodge, T. P.; McLeish, T. C. B. *Macromolecules* **2000**, *33*, 5278.
(55) Cendoya, I.; Alegria, A.; Alberdi, J. M.; Colmenero, J.; Grimm, H.; Richter, D.; Frick, B. *Macromolecules* **1999**, *32*, 4065.
(56) Abtal, E.; Prud'homme, R. E. *Polymer* **1996**, *37*, 3805.

MA021035H